Memristors as Artificial Biochemical Reactions in Cytomorphic Systems

Hanna Abo Hanna*, Loai Danial†, Shahar Kvatinsky†, and Ramez Daniel*
* Department of Biomedical Engineering, † Viterbi Faculty of Electrical Engineering
Technion - Israel Institute of Technology, Haifa 32000 ISRAEL
Email: shahar@ee.technion.ac.il, ramizda@bm.technion.ac.il

***Abstract*— A memristor is a nano-scale two-terminal stochastic electronic device. This paper proposes functional analogies between biochemical reactions and memristive devices. It shows that memristors can mimic biochemical reactions and gene networks efficiently and capture both deterministic and stochastic dynamics at the nano-scale level. We present different abstraction models and voltage-controlled resistive switching circuits that inherently model the activity of genetic circuits with low signal-to-noise ratio (SNR). These findings constitute a milestone for cell-inspired circuit design with noise-tolerance and energy-efficiency features, which can provide a fast and simple emulative framework for studying arbitrary large-scale biological networks in systems and synthetic biology.**

***Keywords*—Cytomorphic, cell-inspired circuits, memristors, molecular biology, synthetic biology, systems biology.**

I. INTRODUCTION

Scientists and researchers have long been inspired by biology and nature when designing novel electronic circuits and systems. An example of such bio-inspired electronic circuits are neuromorphic circuits, which are artificial intelligent systems that share organization principles with the nervous system. Such systems make it possible to integrate models such as the artificial neuron (perceptron) into electronic circuits [1]. Biological systems in living cells can also serve as a source of inspiration, as they perform real-time complex and highly sensitive tasks, and include phenomenally energy-efficient systems. For example, in one second, a cell performs about 10 million energy-consuming noisy chemical reactions, which altogether require about one pico-watt of power, which is much more energy-efficient than any nano-scale digital transistor [1]. Moreover, living cells are fault-tolerant to the highly inherent noise of imperfect and imprecise analog-digital processing parts on its inputs, such that reliable outputs are produced. Therefore, the architectural concepts and design principles of living cells serve as a promising model for novel electronic systems with features similar to those found in the living cells. These cell-inspired circuits are known as *cytomorphic circuits* [1].

Researchers today are further motivated to create simulation and modeling tools which can provide new insights into understanding biological systems and diseases. Biological networks often contain multi-scale, noisy, non-linear, non-modular, and dynamical feedback effects. As such, simulating them is a computationally intensive task. To overcome this challenge, researchers have developed various hardware acceleration techniques that leverage parallelism [2]. However, these techniques have a common drawback: the simulation time inevitably increases as the molecular population size or network scale increases. Hence, new approaches for efficient and high-performance computation are needed to quickly and flexibly simulate and model biological systems. Cytomorphic circuits can abstract the dynamics of biological cells and interpolate their functional properties into electronic systems. Recently, cytomorphic circuits have been used to capture the nonlinearities and stochastic dynamics of biochemical systems to discover pathway parameters, gene regulatory networks, and cell signaling pathways. They have likewise been used to analyze intricate cell functions and to design synthetic circuits [3-5].

In this paper, we propose a novel approach for modeling deterministic and dynamic fluctuations of biochemical reactions and genetic circuits within the cell using memristor-based circuits. Memristive devices are electrical non-linear passive elements that can retain a state of internal resistance based on the history of applied voltage and current. These devices can store and process information by their own conductance [6]. Memristive devices have potential in a wide range of applications, *e.g.*, non-volatile memory, programmable logic, analog computations, and neuromorphic computing, where memristors mimic artificial synapses [7]. Our approach avoids using artificial noise generation circuits, which are normally used to capture the random fluctuations of molecular and genetic circuits that involve a small number of proteins, such as those in DNA-protein binding reactions [1] [3-4]. Noise generation circuits often include analog and digital circuits, which complicate the scaling of cytomorphic integrated electronics.

II. MEMRISTORS MIMIC BIOCHEMICAL REACTIONS

To better understand the motivation for modeling biochemical reactions with memristors, we should begin by examining these reactions in terms of their biophysical dynamics and energy levels. To derive an expression for the reaction rate of a simple biochemical reaction, suppose that P denotes the free chemical species taken to be a protein in this model, N_T is the total number of binding sites, N_{free} is the number of free binding sites, and P^* is the newly formed complex. Such complex formation through a simple binding reaction can be seen as analogous to the ON and OFF states in a memristive device, as illustrated in Fig. 1(a). The dynamics of such binding reactions depend upon the flow (diffusion) of proteins toward the active (free) binding site. As a first order approximation, the reaction rate can be given as:

$$dP^*/dt = k_f \cdot N_T \cdot P, \quad (1)$$

$$N_{free} + P^* = N_T, \quad (2)$$

where Eq. (1) describes the chemical kinetics rate of complex production with rate k_f, and Eq. (2) can be viewed as a molecular balance law. The rate coefficients of such biochemical reactions are exponential in free energy difference and are often described by the Boltzmann statistic

978-1-5386-6378-3/18/$31.00 ©2018 IEEE

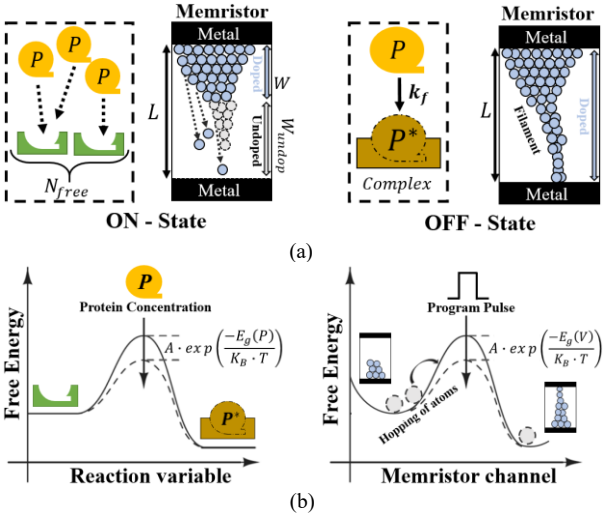

Fig. 1. (a) Analogies between biochemical binding reactions and memristive devices at the nano-scale and biophysical level. (b) Analogies between molecular flux in chemical reactions and ionic species flow in memristive devices.

[1]. Therefore, an increase in enzyme concentration decreases energy barriers, as shown in Fig. 1(b). This process can be seen as analogous to ionic species flow in a memristive device. A simple solution of (1) and (2) shows that the concentration of the new complex P^* can be viewed as two logic levels (zero-ON, and N_T-OFF) [5]. Thus, the biochemical reaction consists of free and occupied binding sites, which can be viewed as time-dependent internal state variables whose sum is constant and which are controlled by protein concentration.

A memristive device built in a metal-insulator-metal structure (Fig. 1) can be generally viewed as two-terminal resistance switches based on ionic motion. The semiconductor thin film within the insulation region has a certain length L and consists of a doped and undoped region [6]. The internal state variable of the memristor w represents the length of the low resistance, doped region (filament length). If the doped region extends to full-length L, the total resistivity of the device will be dominated by a low resistivity region, with a value measured to be R_{ON}. Similarly, when the undoped region, which is represented by $w_{undoped}$, extends to the full-length L, the total resistivity of the device will be dominated by a high resistivity, denoted as R_{OFF}. Switching between the two logic states (R_{ON}/R_{OFF}) is initiated by applying external bias current or voltage across the memristor [6]. The applied current or voltage initiates vacancy migration towards the undoped region, causing the formation of conductive filament as shown in Fig. 1(a). As a first order approximation, the change in the doped region can be described by a linear model:

$$dw/dt = (\mu/L) \cdot R_{ON} \cdot I(t)\,, \tag{3}$$

$$L = w + w_{undoped}, \tag{4}$$

where μ is the mobility of ionic species. Analogous to the rate coefficients in biochemical reactions, the rate of switching in memristive devices follows the Boltzmann statistic and is determined by bias-dependent activation energy [8]. Moreover, an increase in the applied voltage decreases energy barriers (Fig. 1(b)). Therefore, programming pulses and enzyme concentration have similar contributions to the state of memristor and the biochemical reaction, respectively. The equivalency of the equation sets (1,2) and (3,4) reveals the analogy between biochemical reactions and memristor devices in terms of their dynamics. Both systems involve the motion of charged atomic or molecular species, including state variable dependency on time. In addition, the time it takes to form a new complex (binding of protein to binding site or substrate to enzyme) and the delay time of switching memristors both follow a Poisson distribution. Therefore, the stochastic dynamics of biochemical reactions are analogous to the stochastic dynamics of memristor switching. The above-mentioned analogies suggest that large-scale genetic-processing systems in biological networks can be efficiently modeled by hybrid memristor-CMOS electronic circuits.

III. Modeling Michaelis–Menten with Memristors

The kinetics governing biochemical reactions between enzyme E and substrate S is typically given by the Michaelis–Menten equation; this equation is also applicable to a range of other biochemical reactions, such as the binding of proteins to their binding sites within a DNA strand [9]. For thermodynamic reasons, all biochemical reactions proceed in both directions [9], and hence, the kinetics of the complex formation is formulated as:

$$dP^*/dt = k_f \cdot P \cdot N_{free} - k_r \cdot P^*, \tag{5}$$

with k_f and k_r denoting the forward and reverse rate constant, respectively. An illustration of such a reaction between a protein P and a binding site is shown in Fig. 2(a). If the reverse reaction is slow compared to the forward reaction, it is often ignored, and only the primary direction is displayed by (1). Assuming that $P \gg N_{free}$, a solution for (5) and (2) in steady state is:

$$P^* = N_T \cdot \frac{P}{P + K_d}, \tag{6}$$

where $K_d = k_r/k_f$ is known as the dissociation constant and has units of concentration.

Equation (6) can be modeled simply by basic circuit components using Kirchhoff's laws. To model (6) by a KCL circuit, as proposed in [10], one can use a resistive current divider between a memristor with value P and a resistor with a value of K_d, where N_T is the current source and P^* is the current that is passed through the resistor (Fig. 2(c)). Alternately, (6) can be modeled by a KVL circuit, where current dividers are replaced by voltage dividers. Consequently, N_T becomes a voltage source and P^* is the measured voltage on the memristor M_P (Fig. 2(d)). In both configurations, the memristor operates in the analog mode with multiple resistance levels. The memristance is controlled by programming voltage pulses with a constant width. For simplicity, we use a voltage-threshold model to express the memristance [11], which is given by,

$$M_P = (R_{OFF} - R_{ON}) \cdot \frac{w - W_{ON}}{L - W_{ON}} + R_{ON}, \tag{7}$$

$$dw/dt = (\mu/V_T) \cdot (V(t) - V_T), \tag{8}$$

where W_{ON} is the length of the doped region, μ is a constant with units of nm/sec, and V_T is the threshold voltage. For N_p programming pulses with pulse period T_W, and amplitude $A_V > V_T$, the memristance is approximately:

$$M_P = R_{ON} + R_0 \cdot N_p, \tag{9}$$

where $R_0 = (R_{OFF} - R_{ON}) \cdot (\mu/L) \cdot (T_W/V_T) \cdot (A_V - V_T)$. The memristance as in (9) enables us to set the stochasticity of

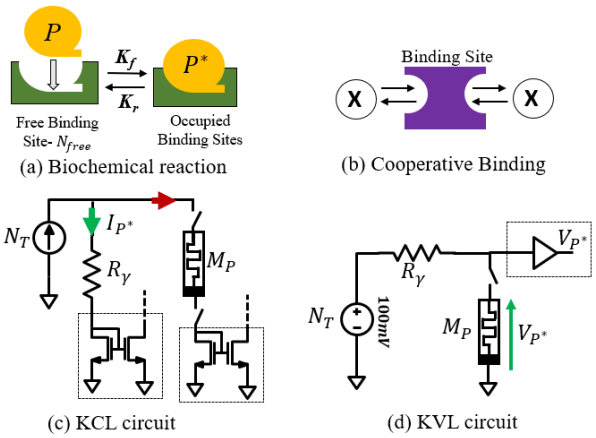

Fig. 2. (a) Simple biochemical reaction between protein $\boldsymbol{P}$ and binding sites $\boldsymbol{N_{free}}$. (b) Cooperative binding between two proteins X and binding site. (c) Memristor based KCL circuit with current mirror. The current through $\boldsymbol{R_Y}$ models complex $\boldsymbol{P^*}$ production. (d) Memristor based KVL circuit with buffer. The voltage on the memristor $\boldsymbol{M_P}$ models complex $\boldsymbol{P^*}$ production. The current mirror and the buffer allow chaining with other stages. Both circuits were designed using the VTEAM memristor model in 0.18um CMOS process.

the memristor by applying a controlled number of pulses following Poisson statistics. This model can be easily extended or replaced by any threshold-based model.

By substituting (9) in the current/voltage divider expressions, the current/voltage passed through the memristor M_P is

$$P^*_{V/I} = N_T \cdot \frac{N_p}{N_p+K_D} + N_T \cdot \frac{R_{ON}}{N_p+K_D}, \qquad (10)$$

where $K_D = R_{ON}/\mathrm{R}_0 + R_Y/\mathrm{R}_0$ is analogous to the dissociation constant, and N_p is analogous to P in (5), which denotes the number of proteins available. The value of K_D can be easily modified by changing the resistor R_Y, or by replacing it with a memristor that is controlled by programming pulses to any desired value. The complex P^* and the total binding sites N_T can be taken as the current or voltage, depending on the circuit. The left-hand term in (10) fits the model of the biochemical binding reaction (6), and the right-hand term is a leakage current/voltage, denoting that even when $N_p = 0$, $P^*_{V/I}$ is not zero. This is known as the basal level inherent in biochemical binding reactions [5].

IV. Genetic Activation and Repression Function

Transcription is the process of converting DNA to mRNA, and it is initiated with the binding of the RNAp enzyme to a specific region in the DNA, also known as the promoter region (Fig. 5). This binding is activated or repressed by biological complexes (proteins), termed activators and repressors, respectively [9]. Activation is modeled by (6), and realized by the KCL and KVL circuits shown in Fig. 2(c-d). Repression is modeled by the concentration of the free binding sites N_{free} and is expressed as

$$N_{free} = N_T - P^* = N_T \cdot \frac{K_D}{P+K_D}. \qquad (11)$$

Equation (11) can be determined by the difference between the total current and the current that is passed through the R_Y resistor in the KCL circuit, or by exchanging the positions of the resistor and the memristor in the KVL circuit. Simulation results for both activator and repressor binding reactions using the KVL model are shown in Fig. 3, while simulation results using the KCL model can be found in [10].

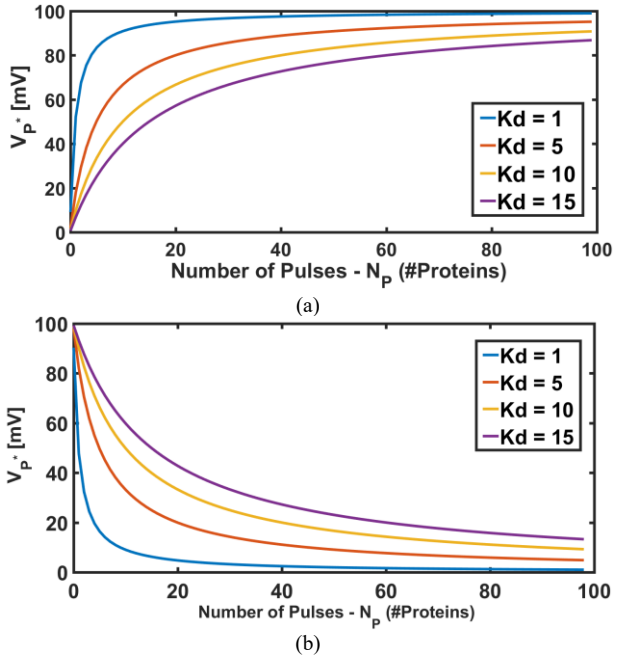

Fig. 3. SPICE simulations of protein binding (activator and repressor), for different values of $\boldsymbol{K_D}$ using the circuit shown in Fig. 3. In this model, the number of pulses $\boldsymbol{N_p}$ is equivalent to the available proteins. (a) Activator concentration and (b) repressor concentration versus $\boldsymbol{N_p}$. Circuit and memristor parameters are summarized in Table I.

TABLE I – Circuit Parameters for Micheles Menten Model

Type	*Parameter*	*Type*	*Parameter*
Memristor	$R_{OFF} = 100K\Omega$ $R_{ON} = 100\Omega$ $L = 10nm$ $\mu = 1mm/sec$ $V_T = 1V$	Dissociation-coefficient $K_d[M]$	$K_d = 1M, R_Y = 1K\Omega$ $K_d = 5M, R_Y = 5K\Omega$ $K_d = 10M, R_Y = 10K\Omega$ $K_d = 15M, R_Y = 15K\Omega$
Pulses	$A_V = 2\,V$ $T_W = 10\,nsec$		

V. The Memristor Captures Cooperativity

A positive "cooperative binding" is known as the ability of proteins to enhance their binding affinity to binding sites by forming a complex that includes identical units [9]. This phenomenon affects the steepness of the protein-DNA transfer function (Eq. (6)). Cooperative binding can be modeled by the Hill coefficient n as

$$P^* = N_T \cdot \frac{P^n}{P^n + K_d}. \qquad (12)$$

If the binding of a protein increases the binding site's apparent affinity, the Hill coefficient will be larger than one (positive cooperativity), and smaller than one if the binding of a protein decreases the apparent affinity (negative cooperativity). Typical values for the Hill coefficient range from $n = 0.5$ to $n = 4$. For $n > 2$, (12) can be described by a digital approximation, using only two states representing a high or low concentration of the formed complex [1]. The digital approximation can be modeled by a memristor operating in the digital mode with only two states: high resistance (R_{OFF}), representing a high concentration ($P^* \approx N_T$), and low resistance (R_{ON}), representing low concentration ($P^* \approx$ basal level). To model cooperativity with $n < 2$, we use the KVL circuit with a memristor exhibiting an exponential dependence on the internal state variable, as follows:

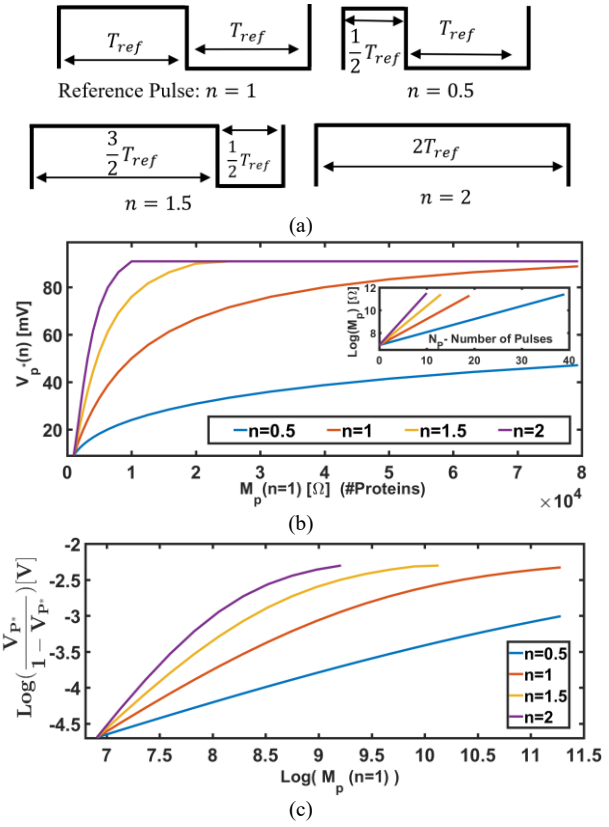

Fig. 4. Simulation results for different Hill coefficients. Circuit and memristor parameters are summarized in Table II. (a) An example of different programming pulses. (b) Simulation results of cooperativity model using the KVL circuit for $\boldsymbol{K_d = 1}$. The inset shows simulation results of the memristance with different Hill coefficients. The slopes indicate the effect of different duty cycles. (c) A typical graph to examine the cooperative binding. The slope of the curves represents the Hill coefficient $\boldsymbol{n}$.

TABLE II - CIRCUIT PARAMETERS FOR COOPERATIVITY MODEL

Type	*Parameter*	*Type*	*Parameter*
Memristor	$R_{OFF} = 100K\Omega$ $R_{ON} = 100\Omega$ $L = 10nm$ $\mu = 1mm/sec$ $V_T = 1V$	Reference Pulse	$A_V = 2\,V$ $T_{REF} = 10\,nsec$ $Duty\ Cycle = 50\%$

$$M_p = R_{ON} \cdot \exp\left(\frac{\lambda}{w_{OFF}-w_{ON}} \cdot (w - W_{ON})\right), \tag{13}$$

where λ is a fitting parameter maintaining $e^{\lambda} = R_{off}/R_{on}$. The exponential dependence allows us to control the memristance slope by changing the duty cycle of the programming pulses with reference to a programming pulse representing $n = 1$. Changing the duty cycle is analogous to multiplying the programming duration by a factor of $n \in \mathcal{R}$, which sets the steepness of the activation function. Examples of such reference and programming pulses are shown in Fig. 5(a). These controlled duty cycle pulses set the memristance M_p in (13), as follows:

$$M_p = R_{ON} \cdot (e^{K \cdot N_p})^n, \tag{14}$$

where $K = \frac{\lambda \cdot \mu}{w_{OFF}-w_{ON}} \left(\frac{A_V - V_T}{V_T}\right) \cdot T_{ref}$. Simulation results representing the change in the M_p slope are shown in the inset of Fig. 4(b). The complex concentration according to the cooperativity model using (6) and (13) is:

$$P^* = N_T \cdot \frac{M_p}{M_p + K_D} = N_T \frac{R_{ON} \cdot (e^{K \cdot N_p})^n}{R_{ON} \cdot (e^{K \cdot N_p})^n + K_D}, \tag{15}$$

where M_p is analogous to P^n in (12). Fig. 4(b) shows the simulation results of (15), using the exponential VTEAM memristor model. The slope of the aforementioned curves is typically examined by plotting a graph of $log(P^*/(1-P^*))$ versus $log(M_p)$, where M_p represents the memristance when the reference programming pulse is used. The graph yields a linear plot with a programmable slope that is proportional to the Hill coefficient. A slope greater than one indicates a positive cooperative binding ($n > 1$), while a slope less than one indicates a negative cooperative binding ($n < 1$) as illustrated in Fig. 4(c) for different values of n.

VI. TRANSCRIPTION-TRANSLATION PROCESS

Biological and electronic systems are inherently stochastic in their behavior. In both systems, the transportation of discrete random carriers is accompanied by collisions and probabilistic arrival, which generate random fluctuations. These fluctuations are known as intrinsic noise through networks and can be described as a Poisson process, generating shot noise (scales as the square-root of the molecular count) [12]. Transcription and translation processes are an example of such stochastic behavior in biology. The expression of mRNA in the transcription process can approximately be viewed as the rate of RNAp arrival at the promoter with variance that is equal to the mean; hence, $\overline{\Delta mRNA^2} = \overline{mRNA}$ [12]. Therefore, we can capture the stochastics of such a process with a pulse counter. Equation (9) shows that a linear memristor under specific conditions can act as an analog counter of the arrival pulses during the programming process. The second stage in Fig. 5 shows a circuit that counts programming pulses arriving to the memristor and represents these programming pulses as the output voltage of a buffer circuit, implemented as a common drain amplifier. In steady state, the buffer output voltage is

$$V_{out_{CD}} = I_M \cdot (M_{RNAp} + R_a) - V_{T0} - \sqrt{I_B / K_0}\,. \tag{16}$$

We define the output v_{mRNA}, which is analogous to the mRNA concentration, as the difference between the voltage for any number of pulses N_R and the voltage for $N_R = 0$ is

$$v_{mRNA} = V_{CD}(N_R) - V_{CD}(N_R = 0) = I_M R_0 N_R\,. \tag{17}$$

Additionally, we define the noise power ψ as the ratio between the variance $\sigma^2_{v_{mRNA}}$ and the mean $\overline{v_{mRNA}}$, and the signal-to-noise ratio SNR as the ratio between $\overline{v_{mRNA}}$ and the standard deviation $\sigma_{v_{mRNA}}$. If the programming pulses N_R are controlled by a "random clock" exhibiting pure Poisson characteristics with mean $\overline{N_R}$ that is equal to the variance $\sigma^2_{N_R}$, the noise power of mRNA production can be expressed as:

$$\psi_{mRNA} = I_M \cdot R_0, \tag{18}$$

and the SNR can be expressed as:

$$SNR_{v_{mRNA}} = \overline{v_{mRNA}} / \sqrt{\overline{\Delta v_{mRNA}{}^2}} = \sqrt{\overline{N_P}}. \tag{19}$$

In this configuration, the number of programming pulses is analogous to the promoter activity, which is controlled by the binding of RNAp to DNA [5]. The formation of mRNA usually begins after some transcription delay time T_D [3]. The delay is a result of the finite velocity at which RNAp moves along the gene during transcription. This delay can be easily

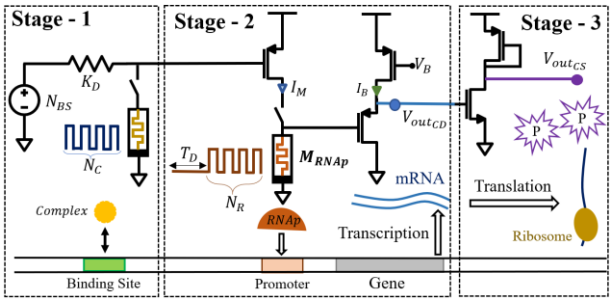

Fig. 5. Memristor based circuit to capture the stochastic behavior of the transcription-transcription process. Stage-1 models the complex binding to a specific binding site by a simple KVL circuit. Stage-2 models the transcription process in which a segment of DNA is copied into mRNA by the enzyme RNA polymerase (RNAp). The arrival of RNAp is modeled by a pulse counter and mRNA production is modeled by a common drain stage. Stage-3 models the translation process by which mRNA is decoded in a ribosome to produce protein. The common source stage models the protein production, while the amplification captures the noise and the burst size in the translation process.

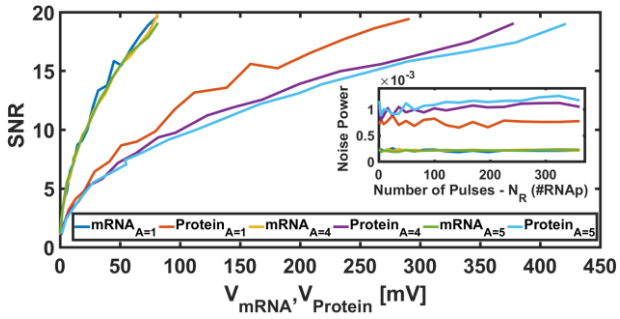

Fig .6. SPICE simulations of SNR versus molecule concentration ($\overline{v_{mRNA}}$, $\overline{v_{Protein}}$) accordingly, for different gains **A** (1, 4 and 5) of the circuit from Fig. 5 with constant I_M. The inset shows simulation results of noise power versus the number of pulses which set the desired SNR.

incorporated into the proposed circuit by lagging the first arrival of programming pulse N_R (Fig. 5). In an analogy to the transcription process, the translation process can be viewed as counting the number of ribosomes that arrive at mRNA molecules, whose stochastic dynamics follows Poisson statistics. Biological experiments and biophysical models show that the noise power in protein production is higher than in mRNA production ($\psi_{protein} > \psi_{mRNA}$). This relation can be described by stating that the variance of protein is larger than the Poisson statistic ($\overline{\Delta Protein^2} = (1+b)\cdot\overline{Protein}$) [12]. The parameter b in biology is known as the burst size and is equivalent to the number of proteins synthesized from a single mRNA transcript [12]. The burst size can be viewed as the molecular gain from mRNA to protein, which amplifies the mRNA noise content in the protein signal. The third stage in Fig. 5 shows a circuit that amplifies the noise of the second stage through a common source (CS) amplifier and captures the burst size and the stochastics of protein production. Similarly, we define the output of the CS amplifier as the difference between the voltage for any number of pulses N_R and the voltage for $N_R = 0$. Thus, the output $v_{protein}$ represents the protein concentration as:

$$|v_{protein}| = (gm_1/gm_2)\cdot I_M \cdot R_0 \cdot N_R. \qquad (20)$$

According to (20), the noise strength in protein production can be expressed as:

$$\psi_{protein} = I_M R_0 \cdot (1+b), \qquad (21)$$

where $1+b \equiv gm_1/g_{m2}$ and can be changed by changing the transistor's width. Simulation results of SNR and noise power for both processes are shown in Fig. 6. Although the transcription process initiates with RNAp binding to the promoter site, the rate of transcription is regulated by other complexes (proteins) that promote or repress the action of RNAp. The first stage in Fig. 5 models the binding of such complexes to the DNA site. The KVL circuit controls and sets the current I_M through a PMOS transistor, thus changing the mRNA and protein signal according to (17) and (20).

VII. Conclusion

We demonstrated the functional analogies between biochemical reactions and memristive devices. We also proposed the adoption of memristors as mimickers of biochemical reactions in cytomorphic systems. Furthermore, we modeled the deterministic and stochastic behaviors of highly noisy genetic systems using memristor-based circuits. These circuits lead towards the design of cell-inspired, energy-efficient electronic circuits that emulate large-scale stochastic biological systems. In our future research, we expect to compare the memristor-based circuits with biological experimental data, and extend the networks to better capture the biological behaviors.

VIII. Acknowlegment

This research was partially supported by the Neubauer Family Foundation, Russell Berrie Nanotechnology Institute NEVET project, the Viterbi Fellowship at the Technion Computer Engineering Center, EU COST Action IC1401 and the Israeli Ministry of Science and Technology.

References

[1] R. Sarpeshkar, "Cytomorphic Electronics: Cell-inspired Electronics for Systems and Synthetic Biology." *Ultra Low Power Bioelectronics: Fundamentals, Biomedical Applications, and Bio-inspired Systems*, Cambridge University Press, Cambridge, U.K. 2010, ch 24, pp. 753– 786.

[2] K. Sumiyoshi, K. Hirata, N. Hiroi, and A. Funahashi, "Acceleration of discrete stochastic biochemical simulation using GPGPU," *Front. Physiol.*, vol. 6, 2015.

[3] S. S. Woo, J. Kim, and R. Sarpeshkar, "A Cytomorphic Chip for Quantitative Modeling of Fundamental Biomolecular Circuits," *IEEE Transactions on Biomedical Circuits and Systems*, Vol. 9, No. 4, pp. 527-542, Aug. 2015.

[4] R. Daniel, S. S. Woo, L. Turicchia, and R. Sarpeshkar, "Analog Transistor Models of Bacterial Genetic Circuits," *Proceedings of the IEEE Symposium on Biological Circuits and Systems*, pp. 333–336, Nov. 2011.

[5] R. Daniel, J. R. Rubens, R. Sarpeshkar, and T. K. Lu, "Synthetic Analog Computation in Living Cells," *Nature*, Vol. 497, pp. 619–623, May 2013.

[6] D. B. Strukov, G. S. Snider, D. R. Stewart, and R. S. Williams, "The Missing Memristor Found," *Nature*, Vol. 453, pp. 80–83, May 2008.

[7] S. H. Jo *et al.*, "Nanoscale Memristor Device as Synapse in Neuromorphic Systems," *Nano Letters*, Vol. 10, No. 4, pp. 1297– 1301, Apr. 2010.

[8] S. H. Jo, K. H. Kim, and W. Lu, "Programmable Resistance Switching in Nanoscale Two-Terminal Devices," *Nano Letters*, Vol. 9, pp. 496–500, Jan. 2009

[9] U. Alon, "An Introduction to Systems Biology: Design Principles of Biological Circuits," *Chapman Hall/CRC Mathematical and Computational Biology Series*, Vol. 10, No. 10. p. 301, 2007.

[10] H. Abo Hanna, L. Daniel, S Kvatinsky, and R. Daniel, "Modeling Biochemical Reactions and Gene Networks with Memristor," *Proceeding of IEEE Biological Circuits and Systems Conference*, pp. 668-671, Dec. 2017.

[11] S. Kvatinsky, M. Ramadan, E. G. Friedman, and A. Kolodny, "VTEAM: A General Model for Voltage-Controlled Memristors," *IEEE Transactions on Circuits and Systems II: Express Briefs*, Vol. 62, No. 8, pp. 786–790, Aug. 2015.

[12] A. Eldar and M. B. Elowitz, "Functional Roles for Noise in Genetic Circuits," *Nature*, Vol. 467, No. 7312, pp. 167–173, September 2010.